GEOLOGICA BALCANICA, 43. 1 – 3, Sofia, Dec. 2014, p. 51-62.

Development of strain fringes in sedimentary rocks: Evidence for deformation of Upper Ordovician glacial diamictites in the western Srednogorie Zone

Athanas Chatalov

Sofia University "St. Kliment Ohridski", 15 Tsar Osvoboditel Blvd., 1504 Sofia; e-mail: chatalov@gea.uni-sofia.bg

(Accepted in revised form: November 2014)

Abstract. The local formation of quartz strain fringes around authigenic pyrite crystals and chamosite strain fringes around detrital grains is described from Hirnantian glaciomarine diamictites (Sirman Formation) of the Palaeozoic Balkan Terrane, now cropping out in the Alpine western Srednogorie Zone. The fringes belong to the antitaxial type and are interpreted as products of synkinematic, low temperature growth in microdilatation sites as a result of diffusive mass-transfer processes. The relatively simple fringe geometry and fiber orientation reflect coaxial progressive deformation that can be broadly related to the Variscan orogeny. Performed XRD analysis of shales intercalated with the diamictites indicates that the Upper Ordovician glacial deposits underwent a high-grade diagenetic alteration. Therefore, this study reports a rare case of development of strain fringes in non-metamorphosed sedimentary rocks.

Chatalov, A. 2014. Development of strain fringes in sedimentary rocks: evidence for deformation of Upper Ordovician glacial diamictites in the western Srednogorie Zone. *Geologica Balcanica*, 43 (1 – 3), 51-62.

Key words: quartz, pyrite, chamosite, strain fringes, diamictites, Hirnantian, Srednogorie Zone.

INTRODUCTION

Some rock microfabrics and microfabric elements reflect deformation and can be used to outline deformation history. For example, dilatation sites result from rearrangement of material by local dilatation and precipitation during deformation (Passchier, Trouw, 2005). These sites include veins, massive strain shadows, fibrous strain fringes, and microboudins. Strain fringes, known also under the genetic term pressure fringes, consist of fibrous material that grows synkinematically between rigid core objects such as coarse crystals or grains, and the surrounding fine-grained matrix. They are usually composed of another mineral than the rigid object and carry information on the deformation history and diffusive mass-transfer processes associated with progressive deformation. Although such microfabrics have been described from various (mostly low-grade) metamorphic rocks, their occurrence in deformed sedimentary rocks (mainly sandstones and marlstones) has been rarely reported (Ramsay, Huber, 1983; Liu, 2002; Meere, Mulchrone, 2006).

The present study deals with the local formation of quartz strain fringes around authigenic pyrite crystals and chlorite strain fringes around clastic grains in glaciomarine diamictites of Late Ordovician age from the western Srednogorie Zone. Three main items can be pointed out as outlining the aims of this paper: a) to document a rare case of development of strain fringes in sedimentary rocks; b) to characterize the fabric of these specific deformation products and identify their mineralogy; c) to discuss the general conditions and possible time constraints on their formation. In connection with the first task pilot samples from shales were also analyzed to determine the post-depositional degree of alteration of the Upper Ordovician rocks.

GEOLOGICAL SETTING

Ordovician metamorphic and sedimentary rocks are exposed over a large area in the western part of Stara Planina Mountains, to the west and east of Iskar River valley, being part of the Palaeozoic Balkan Terrane (Yanev, 2000; Yanev et al., 2005). The approximately 1800 m thick sedimentary marine succession consists of argillites, siltstones and sandstones plus minor amount of chert and sporadic oolitic ironstones (Yanev, 2000; Gutiérrez-Marco et al., 2003; Yanev et al., 2005). In terms of tectonic subdivision of the Alpine orogen, the Ordovician rocks belong to the Svoge Unit (Fig. 1) which represents an allochthonous tectonic unit in the western part of the Srednogorie Zone (Ivanov, 1998). The pre-Mesozoic basement of the Svoge Unit was greatly influenced by pre-Alpine and Alpine deformations (folding, faulting, and thrusting) that occurred in several stages (Ivanov, 1970; Tsankov, 1995).

The uppermost part of the Ordovician system comprises a siliciclastic succession and the basal strata of an overlying clayey-cherty succession referred to as Sirman Formation and Saltar Formation, respectively (Sachanski, Tenchov, 1993) (Fig. 2). Hirnantian age was proved for deposits of the former unit on the basis of determined graptolites and palynomorphs from the lowermost levels of Saltar Formation (Sachanski, 1993; Lakova, Sachanski, 2004). Non-fossiliferous rocks of the underlying Tseretsel Formation correspond to the Katian stage as defined by their stratigraphic position (Sachanski, 1994).

The thickness of Sirman Formation ranges between 7 m and 10 m. Its lithology includes diamictites of glaciomarine origin and intercalated beds of inter-glacial shales (Sachanski, 1994; Chatalov et al., 2014). According to Sachanski (1994), the deposition of diamictites resulted from extensive glaciation and subsequent ice melting across the Gondwana palaeo-continent and the related global sea-level fall and rise during the Hirnantian. Palaeoclimatical interpretations suggest palaegeographic position of the depositional environment in the temperate humid zone at about 40° of south latitude (Yanev, 2000; Gutierrez-Marco et al., 2003; Yanev et al., 2005). Recently, Chatalov et al. (2014) have presented macro- and micropetrographic evidence for glaciomarine origin of the Hirnantian strata assigning them to an ice-distal facies.

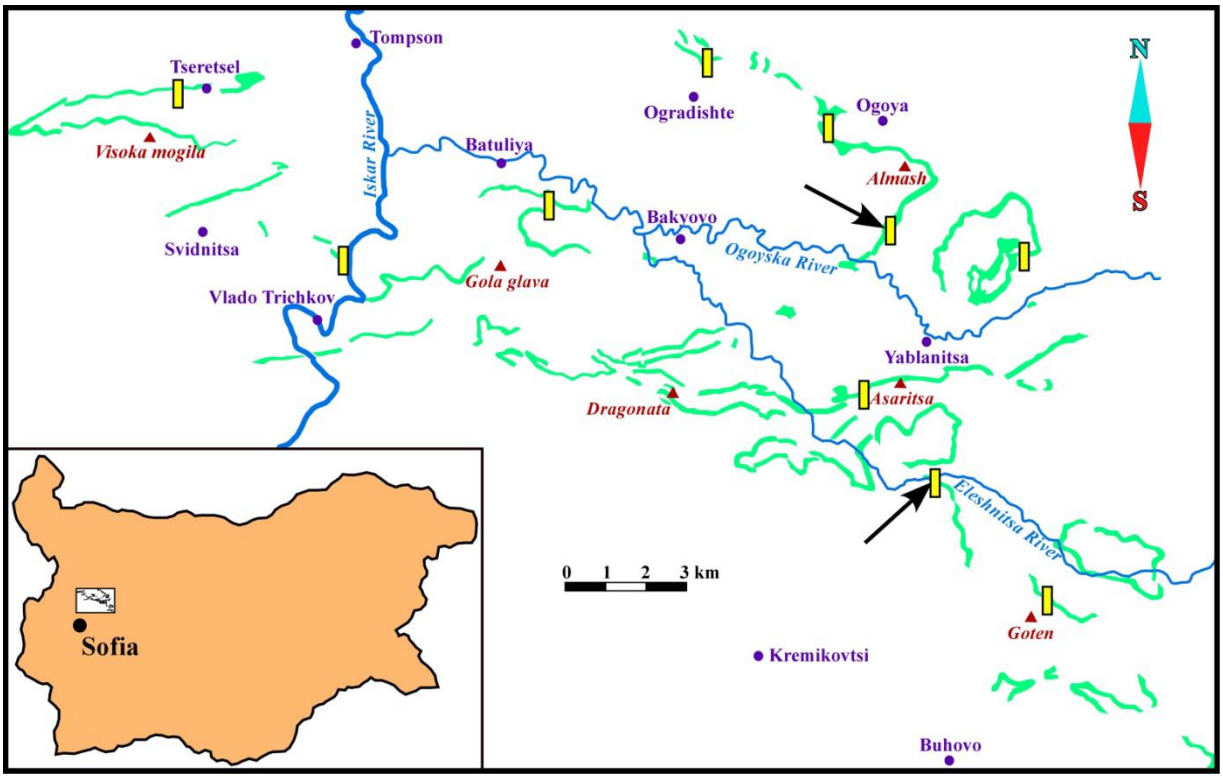

Fig. 1. Surface occurrence of the Upper Ordovician to Llandovery sedimentary rocks of Sirman Formation and Saltar Formation in the Svoge Unit of Srednogorie Tectonic Zone (after Angelov et al., 2010, 2011) with designated locations (rectangles) of the studied sections of Sirman Formation. The upper arrow points to the Govedarski dol section and the lower arrow points to the Eleshnitsa section. Note: The small outcrops in the vicinity of Shuma village (Godech region) are not shown on the map.

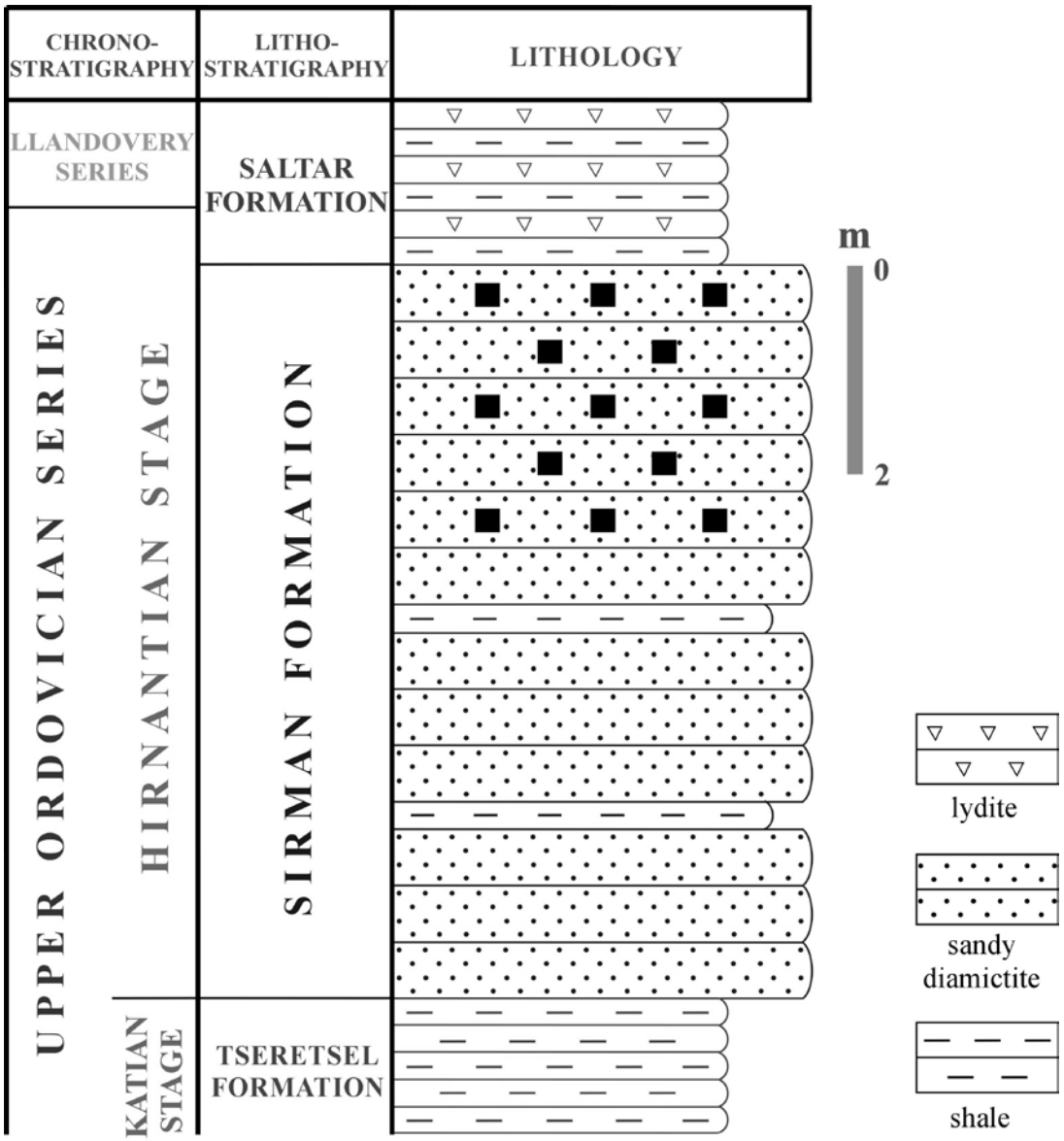

Fig. 2. Stratigraphic-lithologic log of the Hirnantian sedimentary succession in the Eleshnitsa section. Black squares show the vertical occurrence of pyrite crystals/aggregates with developed quartz strain fringes.

MATERIAL AND METHODS

Ten stratigraphic sections with Hirnantian rocks were selected for description and sampling in the field as part of a sedimentological research (Fig. 1). Fifty-two samples from diamicitites and shales of the Sirman Formation were collected for observation with transmitted light microscopy and laboratory analyses. Thin sections were prepared from all samples that were taken with transverse orientation to bedding. Slabs of diamictites showing the massive development of authigenic pyrite were polished to reveal the relationships of this mineral with depositional laminae.

X-ray diffraction (XRD) was applied to determine the diagenetic/metamorphic grade of the Upper Ordovician rocks by analyzing three pilot samples collected from shales. The whole rock samples were first dried and crushed to fine powder. Then the <2 μm fraction was separated after differential settling of coarser particles and oriented aggregates were prepared by sedimentation of suspension on glass slides. The powder XRD patterns of air-dried and ethylene-glycol treated samples were recorded by using TUR M62 diffractometer (Sofia University "St. Kliment Ohridski") with filtered Co Kα radiation in the 4–80^{o} 2θ range at a scan speed of 2 seconds per step of 0.01^{o} 2θ. The bulk clay mineralogy, expandability measurements (% of illite in illite/smectite) and Reichweite ordering values (R) of mixed-layer I/S were determined according to the methodology proposed by Moore,

Reynolds (1997).

Double-polished thin sections were prepared from two diamictite samples displaying phyllosilicate fringes around detrital sand grains. The mineralogy of these fringes was identified by means of quantitative microprobe analysis after vacuum-coating in carbon using scanning electron microscope JEOL Superprobe 733 equipped with EDS HNU 5000 (Geological Institute, BAS). Analytical conditions were 20 kV accelerating voltage, 2.10^{-9} Å beam current and 1 μm spot size. The following JEOL calibration standards were used: quartz for Si, TiO_2 for Ti, Al_2O_3 for Al, Fe_2O_3 for Fe, MnO_2 for Mn, MgO for Mg, apatite for Ca, albite for Na and K-feldspar for K.

PETROGRAPHY OF THE DIAMICTITES

The Hirnantian diamictites are dark grey, medium-bedded to thick-bedded rocks showing commonly massive structure. Horizontal lamination is observed in some beds forming upper levels of the Sirman Formation (Fig. 3). The macrofabrics are dominated by sand-sized detrital grains defining the rocks as sandy diamictites (Chatalov et al., 2014). The latter also contain granules and pebbles of dark grey and grey-greenish shales having diverse shapes and degrees of roundness. Under the microscope, the rocks display poorly sorted texture comprising sand-sized to granule-sized clastics and muddy matrix (Figs. 4, 5). The former are represented by abundant mono- and polycrystalline

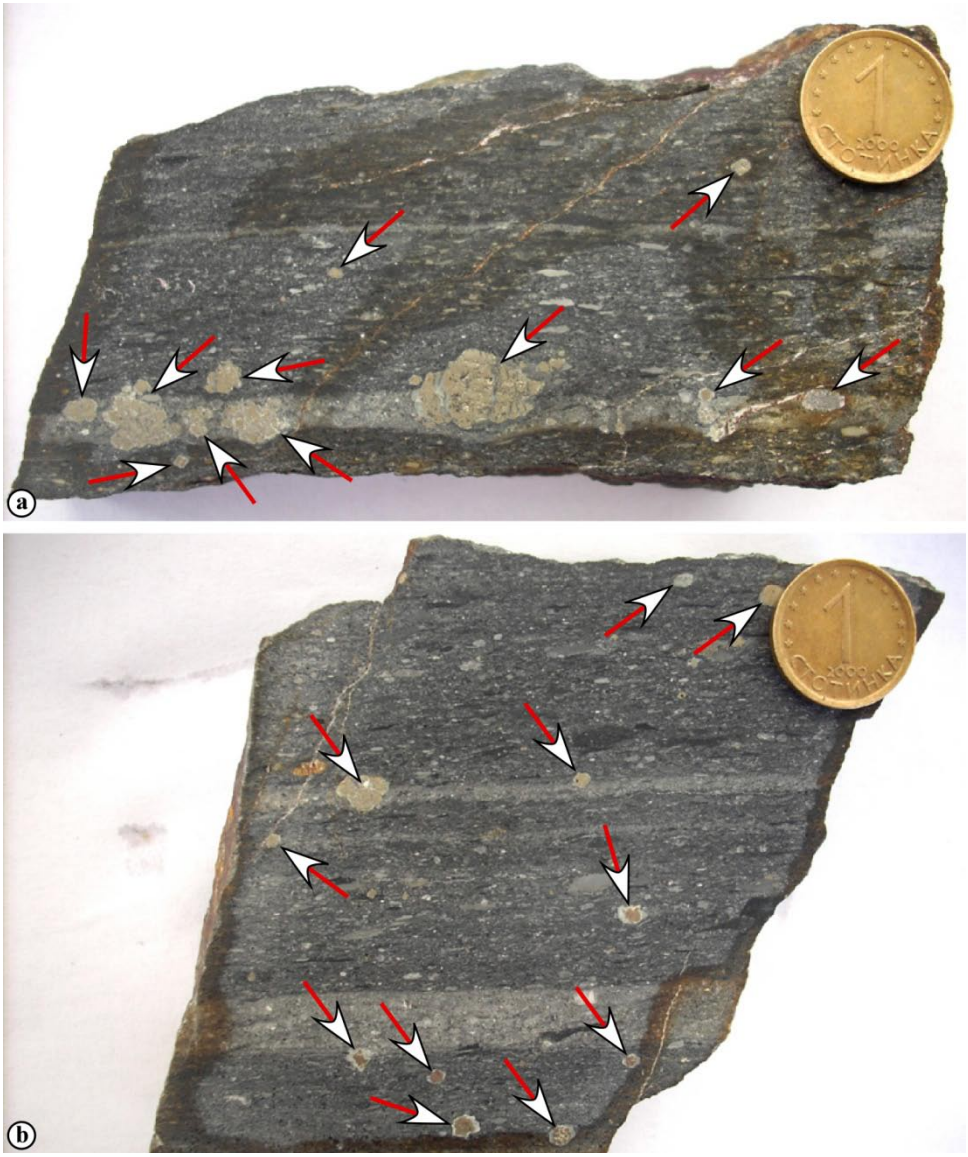

Fig. 3. a, b – Polished slabs of laminated sandy diamictites from the Eleshnitsa section showing authigenic pyrite crystals/aggregates with various sizes (larger ones marked with arrows) that commonly crosscut the depositional laminae. Thin halos of whitish quartz, i.e. strain fringes, are well visible around some of the pyrite crystals/aggregates. Coin diameter is 15 mm.

quartz (≥80%), subordinate lithoclasts (10-20%), single grains of feldspar and heavy minerals (zircon, tourmaline, and rutile), plus scarce flakes of white mica. The detrital constituents vary from subangular to well rounded and show various degrees of sphericity. Some morphological and optical characteristics of the monocrystalline quartz grains imply provenance related to different sources. Extrabasinal clasts were derived from sandstones, siltstones, claystones, quartzites, and microcrystalline chert. Many lithoclasts display diagnostic features of intrabasinal components, e.g. diffuse boundaries, pronounced anisometric shapes, traces of soft deformation and fabrics closely resembling the rock matrix. The latter consists of low birefringent clay particles and silt grains dominated by angular quartz. The diamictites are characterized by random orientation of the anisometric detrital grains and phyllosilicate particles in the matrix.

DESCRIPTION OF THE STRAIN FRINGES

Macroscopically, pyrite crystals and aggregates were locally observed in the upper part of Sirman Formation being most abundant in sandy diamictites from the section located in Eleshnitsa River valley (Figs. 1, 2). They have various sizes from <1 mm to about 1 cm and commonly crosscut the depositional laminae which is well visible in polished slabs (Fig. 3). The bulk of those crystals/aggregates are surrounded by whitish quartz halos that are recognized in thin sections as forming monomineralic fibrous fringes. Under the microscope, the discrete pyrite crystals display sections of subhedral to euhedral forms indicating cubic, octahedral or pyritohedral habits with smooth or rough surfaces. The quartz fringes have lengths from a few tens of microns to 0.25 mm showing normal or oblique orientation of the individual fibers to the pyrite substrate (Fig. 4a). In most cases the fringes overgrow all faces of the pyrite euhedra (Fig. 4b) but elsewhere they are not developed on some of their sides (Fig. 4c). The smaller pyrite crystals (0.05-0.2 mm) have conspicuously thinner overgrowths (Fig. 4d). The fibrous fringes show non-isopachous pattern and sharp boundaries with the adjacent diamictite matrix. However, the length of a given fringe is nearly constant in the sector that is linked to a particular crystal face/side of pyrite. Locally, two pyrite crystals may share a common fringe (Fig. 4e). Fibrous quartz is also observed between contiguous parts of large fractured pyrite crystals while the associated fine-grained pyrite (<0.05 mm) is almost devoid of fringes (Fig. 4f). Inclusions of quartz sized up to 0.2 mm occur within all pyrite crystals that are coarser than 0.05 mm. Few of those inclusions show fibrous fabric having the same orientation of fibers as in the closest sector of the fringe (Fig. 4g). The elongated quartz crystals forming fringes have mostly subparallel arrangement relative to one another. In some places they show minor deviation from their commonly straight orientation (i.e. palisade pattern) outlining slight curvature in the distal parts of the fringes (Fig. 4h). The width of individual quartz fibers is variable and the crystal morphology ranges from fibrous acicular (width <10 μm) to fibrous columnar (width >10 μm). The inclined extinction and positive elongation of the quartz crystals, i.e. c-axis oriented at approximately 30° to the long axis of the fibers, defines the optical variety of length-slow chalcedony known as lutecite.

Locally developed aggregates of another fibrous mineral were observed under the microscope in a few samples of sandy diamictites collected from the Govedarski dol section (Fig. 1). These aggregates display normal or oblique orientation to the substrate which is represented by sand-sized clastic grains of mono- and polycrystalline quartz, or extraclasts derived from quartzites and quartzose sandstones. The individual crystals are colourless in plane light showing fibrous acicular morphology, i.e. with high length/width ratio and width <10 μm (Fig. 5a). In polarized light the mineral shows low birefringence with first-order grey interference colour (Fig. 5b). The fibers commonly form bridges between two adjoining detrital grains as the discrete acicular crystals have subparallel orientation relative to one another (Fig. 5c). The length of these fibrous bridges varies from several tens of microns to 0.3 mm being entirely predetermined by the distance between the respective substrate grains. Longer bridges between large grains may enclose tiny corroded quartz grains which do not disturb the uniform straight orientation of the fibers (Fig. 5d). Elsewhere, the fibrous aggregates growing on a large grain terminate against a few smaller clastic grains and locally may show some deformation in their distal part (Fig. 5e). Within a certain sector of the rock a number of closely spaced detrital grains are connected with several bridges that have subparallel orientation of their fibers (Fig. 5f). The sporadically unilateral growth of fibrous aggregates on substrate grains is characterized by a fringe reaching only some of the closest clastic grains (Fig. 5g) as a sharp boundary is outlined between that fringe and the adjacent clayey matrix (Fig. 5h). Fibrous aggregates are rarely observed between tiny quartz grains and do not occur between distant grains separated by abundant matrix. Also, fringes are not developed on shale lithoclasts, feldspar grains, heavy minerals, and mica flakes. In general, the substrate detrital grains with fibrous overgrowths retain their surface roundness inherited from the stages of transport and deposition, but locally may demonstrate well visible effects from pressure solution, e.g. pitted edges (Fig. 5d).

CHEMICAL COMPOSITION OF THE FIBROUS FRINGES

While the quartz fringes around pyrite crystals are easily recognized in the thin sections, the other fibrous mineral forming overgrowths on clastic grains was identified by

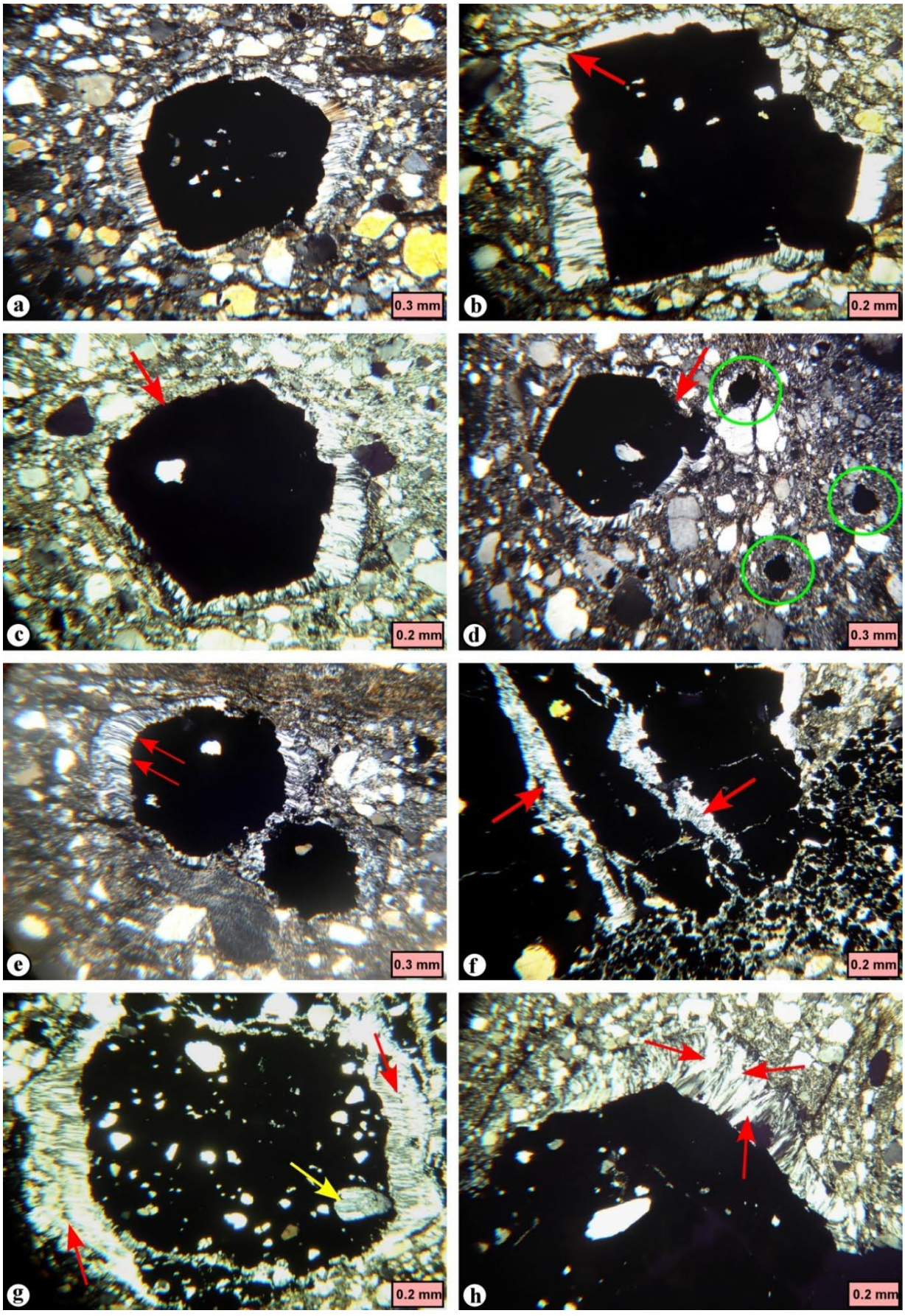
a
0.3 mm
b
0.2 mm
c
0.2 mm
d
0.3 mm
e
0.3 mm
f
0.2 mm
g
0.2 mm
h
0.2 mm

Fig. 4. Late diagenetic subhedral to euhedral pyrite crystals with non-isopachous strain fringes of fibrous quartz (lutecite): a, b – Face-controlled and displacement-controlled fringes overgrowing the entire pyrite substrate and showing sharp boundaries with the adjacent diamictite matrix. The length of a discrete fringe is nearly constant in the sector that is linked to a particular crystal face. The dependence between roughness of the core object surface and the respective type of fringe growth is clearly demonstrated. Note the planar line separating fibre aggregates in the face-controlled fringes on two neighbouring faces of the pyrite cube (arrow); c, d – Fringes overgrowing most sides of the pyrite crystals but not developed on some faces (arrows). The associated smaller pyrite crystals (encircled) have conspicuously thinner overgrowths; e – Two adjoining pyrite crystals sharing a common fringe and showing enhanced fringe growth around the larger core object. Individual fibers (arrows) retain constant crystallographic orientation in the slightly curved distal part of the left fringe; f – Fibrous quartz (arrows) growing between contiguous parts of a large fractured pyrite crystal. The associated fine-grained pyrite is almost devoid of strain fringes; g – Displacement-controlled fringe composed of two growth increments (boundary shown with red arrows). One large inclusion in the pyrite (yellow arrow) displays fibrous fabric with its individual crystals having the same orientation as in the closest sector of the strain fringe; h – Fringe with locally curved fibers whose low temperature rigid growth is evidenced by the lack of undulose extinction (arrows) and effects of dynamic recrystallization. Note: All microphotographs in polarized light.

means of chemical analysis. The obtained results record similar values of the major oxides defining chlorite compositions (Table 1). The structural formulae of chlorites were calculated considering 28 negative charges and ferrous iron. Small amounts of potassium are interpreted as indicative of illite contamination. According to the dominant divalent octahedral cation in the structural formula and the measured Fe/Fe+Mg ratio (0.69–0.73), the analyzed chlorite corresponds to magnesian chamosite.

INTERPRETATION AND DISCUSSION

A comprehensive literature review on the Palaeozoic sedimentary rocks exposed in NW Bulgaria shows different views regarding their post-depositional change. For example, the Upper Ordovician strata were considered in most geological works as non-metamorphosed sediments (e.g., Sachanski, Tenchov, 1993; Yanev et al., 2005). However, Yanev, Stefanov (2001) concluded that all Palaeozoic pelitic rocks of Western Stara Planina Mountains were affected by very low-grade metamorphism (i.e. anchimetamorphic conditions) as their statement was based on analysis of the Kübler index of illite crystallinity. The performed XRD study of pilot samples from shales of the Sirman Formation reveals the massive presence of kaolinite and partly ordered R=1 illite/smectite with illitic layers in the range of 65-75%. Because the almost complete absence of kaolinite and expandable layers (<10%) in ordered (R>1) illite/smectite is used as diagnostic characteristic to define the anchizone range (Merriman, Peacor, 1999; Perri, 2008), these results indicate that the Upper Ordovician deposits underwent a high-grade diagenetic change during burial. Moreover, the lack of slaty or "rough" cleavage (Durney, Kisch, 1994) types, demonstrated by fine-grained phyllosilicates and detrital grains in the diamictites (Figs 4a, 5a) and associated shales, also conforms to a late diagenetic post-depositional history. Therefore, the described strain fringes developed as a result of deformation of non-metamorphosed sedimentary rocks.

While framboids and small euhedra are the dominant pyrite morphologies found in sediments, coarser pyrite crystals are recognized in ancient sedimentary rocks suggesting late diagenetic origin (Goldhaber, 2005). Most late diagenetic pyrite is formed in a closed system with limited sulfate availability and the particular pyrite morphology is a function of the degree of supersaturation of the solution. The coarse crystal size, crosscutting relationships to depositional laminae, clear replacement pattern, predominant euhedral habit and lack of evidence for metamorphic alteration suggest late diagenetic pyrite formation in the Hirnantian glaciomarine diamictites.

The observed fringes of fibrous quartz around euhedral pyrite crystals belong to the antitaxial type, also known as pyrite-type fringes (Ramsay, Huber, 1983; Passchier, Trouw, 2005). These most frequently reported strain fringes in the literature usually consist of fibrous quartz, calcite and/or phyllosilicates that develop on rigid mineral grains (core objects) such as pyrite or magnetite crystals. When subjected to progressive deformation the soft fine-grained matrix tends to flow away from the rigid object because the latter extends more slowly. Thus, the core objects in a ductilely deforming rock cause local perturbations of the stress field and flow pattern resulting in rearrangement of material in response to inhomogeneous deformation of the surrounding matrix. In the case of low temperature deformation and high fluid pressure, increased pressure solution may occur adjacent to the rigid object on the side of the shortening instantaneous stretching axis (ISA), while gashes may open on the contact between the core object and the matrix on the side of the extensional ISA. Such process creates zones of anomalously low pressure and material migrates towards these zones by fluid advection, i.e. transport from outside in an open system, or by fluid-enhanced diffusion, i.e. derived from the surrounding wall rock in a closed system. The growth of crystalline

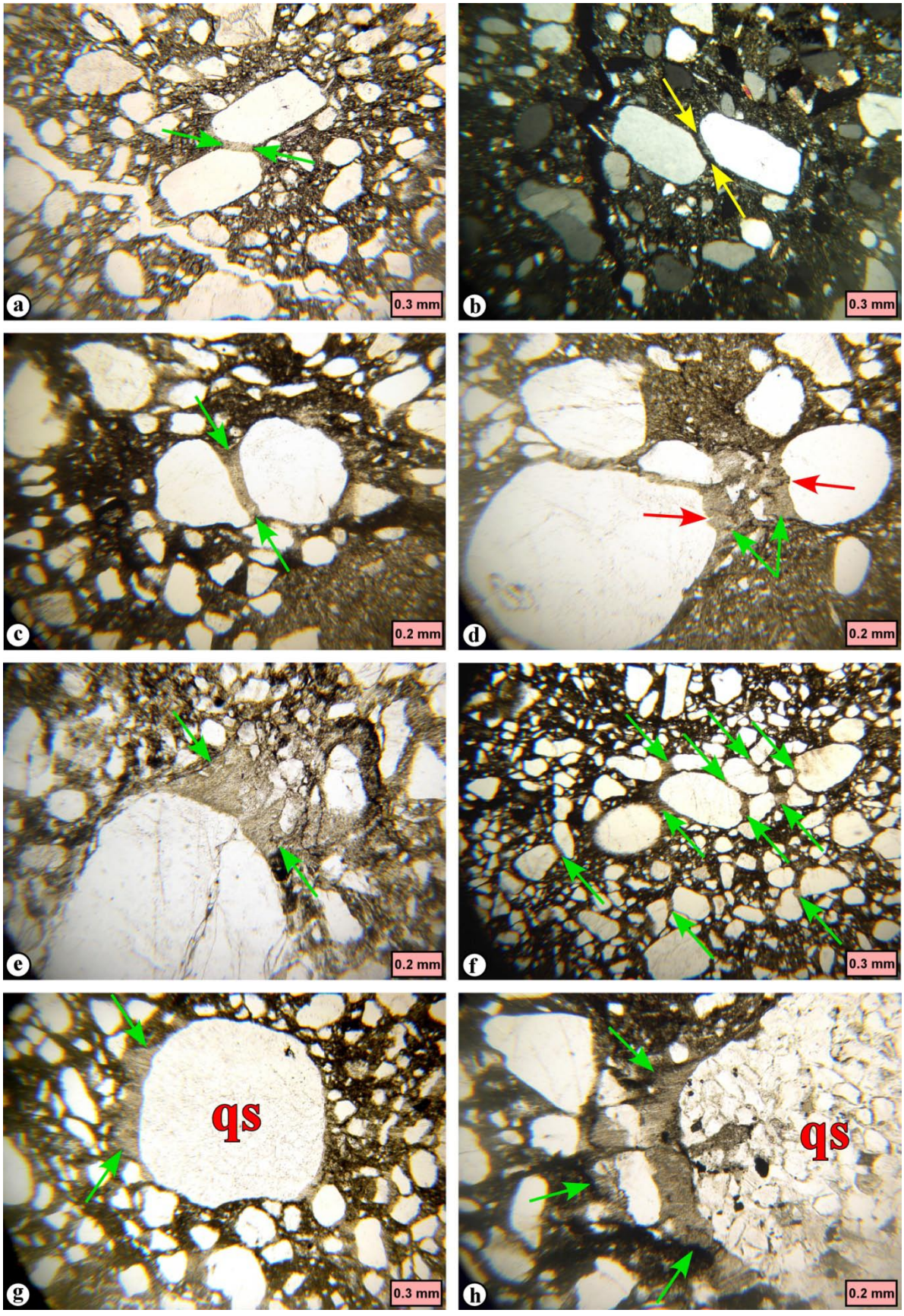
a
0.3 mm
b
0.3 mm
c
0.2 mm
d
0.2 mm
e
0.2 mm
f
0.3 mm
qs
g
0.3 mm
qs
h
0.2 mm

Fig. 5. Strain fringes (beards) of fibrous chamosite developed on clastic grains: a – Colourless fibrous aggregate bridging (arrows) two quartz grains; b – The same object showing low birefringence with first-order grey interference colour of the chamosite (arrows); c – Acicular crystals with subparallel orientation (arrows) growing normally on two adjoining quartz grains; d – Long and thick fibrous bridge (coupled green arrows) between two large quartz grains enclosing several tiny quartz grains without disturbance of the uniform orientation of the fibers. Pitted surface of the substrate (red arrows) and corrosion of the entrapped grains indicate effects from pressure solution; e – Fibrous aggregate (arrows) growing on large quartz grain and terminating against a few quartz grains of smaller size. Some deformation in the distal part of the strain fringe is visible; f – Closely spaced quartz grains connected with several chlorite bridges that have subparallel orientation of their fibres (arrows). Note the absence of chamosite aggregates between the smaller detrital grains as well as between distant grains separated by abundant matrix; g – Strain fringe (arrows) showing preferential growth on the left side of extraclast from quartzose sandstones (qs) and reaching only some of the closest clastic quartz grains; h – Sharp boundary (arrows) between chamosite beard developed on extraclast of quartzose sandstones (qs) and the adjacent clayey matrix. Note: All microphotographs in plane light (except b – polarized light).

material in the gashes forms strain fringes on opposite sides of the core object. These antitaxial fringes grow with crystallographic continuity from the matrix grains towards the rigid object, i.e. the growth surface is between the fringe and the core object. Crystals building the strain fringes are usually fibrous due to their anisotropic growth kinetics and minor or no growth competition.

The geometry of strain fringes depends on the shape of the core object, its initial orientation with respect to kinematic axes and the roughness of its surface (Passchier, Trouw, 2005). Other factors include flow regime in the surrounding matrix, the particular type of strain fringe, and whether the fibre growth is face-controlled or displacement-controlled. While face-controlled fibers grow perpendicular to the growth surface, displacement-controlled fringes track the separation of the matrix from the core object irrespective of the orientation of the latter (Ramsay, Huber, 1983). If the core object surface is smooth, face-controlled fibres tend to develop growing towards the object surface, independently of the relative motion of fringe and object. Fringe structures with both displacement-controlled and face-controlled fibers grow preferentially on rough core objects (Koehn et al., 2000). In this study, some quartz strain fringes reflect face-controlled growth which is best seen on the smooth flat faces of cubic pyrite crystals (Fig. 4b). Displacement-controlled fringes are also widely developed lying oblique to the core object/matrix interface (Fig. 4d, e, g). Elsewhere, face-controlled, displacement-controlled and so called intermediate fibres coexist around pyrite euhedra, or in fringes formed within fractured pyrite crystals (Fig. 4a, c, f, h). In most cases the dependence between roughness of the core object surface and the respective type of fringe growth is clearly demonstrated.

The fibres of strain fringes may be deformable under high temperature conditions, or rigid under low temperature conditions (Ramsay, Huber, 1983). The observed quartz fringes show that they behaved as relatively rigid masses during their growth compared to the surrounding matrix. Their non-deformed pattern can be recognized by a “cast” of the core object at the distal part of some longer fringes (Fig. 4a, g), straight orientation and subparallel arrangement of the individual fibers (Fig. 4c, d), perpendicular relationships of neighbouring fiber groups in the face-controlled fringes on pyrite cubes (Fig. 4b), and the lack of undulose fiber extinction and effects of dynamic recrystallization (Fig. 4h). Also, in the rarely occurring fringes with more than one growth increment the fiber length is greatest in the latest developed increment (Fig. 4g), as was illustrated in Figure 14.15 of Ramsay, Huber (1983). Only locally displacement-controlled and face-controlled fringes are slightly curved in their distal part (Fig. 4e, h). This little change in the fiber orientation from their inner (younger) to their outer (older) part indicates minor rotation between the core object and the fringe. However, the individual fibers retain a constant crystallographic orientation, and hence, the curvature is probably a growth feature and not the result of late deformation of previously straight fibers (Ramsey, Huber, 1983).

The lack or poor development of strain fringes around smaller pyrite crystals (Fig. 4d, f) might be explained with later formation of those crystals relative to the coarse pyrite, i.e. postdating the deformation event (cf. Ghosh et al., 2013). However, enhancement of the fringe growth around larger core objects can be inferred from other thin sections where adjoining pyrite crystals with different sizes display fringes with different lengths (Fig. 4e). A few large core objects have fringes that are not developed on one of their sides or crystal faces (Fig. 4c, d). According to Bons et al. (2012), which parts of the object actually experience a net extension and subsequent fringe formation depends on its shape, the stress field and the fluid pressure. These factors control whether the fringe develops around the entire core object, or only along a part, or even only on one side. The rare occurrence of fibrous quartz inclusions in pyrite crystals is spectacular (Fig.

4g) implying that some parts of the matrix became entrapped during the pyrite growth process and subsequently underwent the same change as the deforming matrix on the nearest outer side of the core object.

The relatively simple fringe geometry and fiber orientation together with the absence of complex S-shaped and Z-shaped fringes suggest coaxial progressive deformation. Thus, they correspond to the theoretical models and computer simulations for development of face-controlled and displacement-controlled fibres around smooth cubic and rough round core objects in pure shear flow (see Koehn et al., 2000, Fig. 6; Passchier, Trouw, 2005, Fig. 6.22). This conclusion is also supported by the subplanar partition surfaces (also named as contact sutures or suture lines by Ramsay, Huber, 1983) which separate differently oriented fibre aggregates in face-controlled fringes on adjacent faces of cubic pyrite euhedra (Fig. 4b), thus indicating a non-rotational deformation during the fibre growth.

The chamosite aggregates developed around clastic grains in the sandy diamictites resemble the characteristics of so called mica beards. The latter are a distinctive type of strain fringe consisting of fibrous mica sometimes associated with other minerals such as chlorite and quartz (Means, 1975). Mica beards define a specific shape fabric in which the fibers are oriented perpendicular to the original direction of maximum pressure, i.e. parallel to the direction of extension. They grow in microdilatation sites as the matrix progressively pulls away from rigid objects during stretching. These peculiar fringes form by diffusion mass transfer of chemical components in aqueous solution (i.e. stress-induced solution transfer, also termed as pressure solution) as material is dissolved from sites of high normal compressive stress and redeposited in low strain zones. Mica beards are common on detrital quartz and other rigid grains (feldspar, lithoclasts) in deformed low-grade metamorphic rocks, e.g. slates, metasandstones, schists (Williams, 1972; Means, 1975; Gray, 1978; van der Pluijm, 1984) but have also been described as projecting out from porphyroblasts in high-grade rocks, e.g. mylonites, amphibolites, gneisses (Lafrance, Vernon, 1998; Wintsch, Yi, 2002). Only few occurrences of beards with presumably illite or chlorite mineralogy have been reported from non-metamorphosed sandstones (e.g. Liu, 2002; Meere, Mulchrone, 2006).

The observed strain fringes correspond to diagnostic features of mica beards including elongated habit of the phyllosilicate aggregates, consistent orientation of the individual fibres, and uniform composition (Fig. 5b). The latter characteristic suggests that the chamosite fringes grew from a common solution, and hence, are not the product of local replacement or recrystallization of detrital grains and/or matrix. Phyllosilicates in the host rock played the role of nuclei for chlorite nucleation in a crack which formed at the contact between the substrate clastic grain and the matrix, i.e. the fringe is younger toward the host rigid grain indicating antitaxial growth (van der Pluijm, 1984). The same conclusion is inferred from the sharp boundary between the strain fringe and the adjacent rock matrix (Fig. 5h). The chamosite beards are either asymmetric, i.e. showing unilateral growth on the substrate, or clearly symmetric, i.e. developed on both sides of the detrital grain. Some controlling factors on the particular type of fringe growth include substrate mineralogy, size of the rigid object, and distance between the clastic grains (Gray, 1978). Thus, chamosite beards developed solely on quartz and quartz-bearing grains, and enhancement of the fringe growth around larger grains is clearly observed (Fig. 5a, c). The most favourable sites, i.e. low strain zones, were between relatively large quartz grains separated by small amount of matrix as the latter promoted stress-induced solution transfer by water film diffusion. By contrast, floating detrital grains are not connected by fibrous bridges because abundant clay retards pressure solution (Dewers, Ortoleva, 1991). In some sectors of the rock the almost linear concentration of chlorite beards with subparallel orientation of their fibers around closely spaced quartz grains is evidence for stress-induced solution transfer and fringe growth parallel to the direction of extension (Fig. 5f). The pitted and corroded surfaces of larger substrate grains and smaller quartz grains entrapped in the fringes likewise reveal effects of pressure solution (Fig. 5d). The generally non-deformed pattern of the fringes suggests their relatively rigid low-temperature growth which can be recognized by the straight orientation of fibers and the lack of effects of dynamic recrystallization (Fig. 5g). Only locally the fibres are slightly curved in their distal part (Fig. 5e), implying some heterogeneity in the local deformation and minor rotation between the substrate grain and the fringe.

In general, the composition of beards is similar to that of the rock matrix reflecting their formation in a geochemically closed system (Gray, 1978). Chamosite is a Fe-rich chlorite that is typically formed during burial diagenesis under reducing, post-oxic conditions (Young, Taylor, 1989). The possible mechanisms include interaction between available kaolinite and iron oxides, transformation of precursor berthierine, and/or formation related to the smectite-to-illite reaction (i.e. release of Fe and Mg as by-products). Similarly to the above described quartz fibers, the chamosite crystals nucleated from matrix particles which were of the same mineral species, i.e. chlorite, or had some chemical affinity with composition of the fibers, e.g. other clay minerals. Although the clay mineralogy of the sandy diamictites was not determined by means of XRD because of the very high amount of quartz, bulk chemical analyses reveal relatively high percentage of FeO (1.99–8.40%) and MgO (0.73–4.38) in these rocks (Chatalov, unpublished results). Moreover, the presence of kaolinite, chlorite and illite/smectite in the associated shales recorded by the XRD analyses is consistent with

a favourable source of chemical components for the authigenic growth of chamosite strain fringes. It is noteworthy that Fe-rich chlorite was considered by some authors as typical of cool-to-cold climatic conditions and may be the dominant clay mineral in Arctic seas sediments depending on the intensity of weathering in the source areas. Chamosite formation was likewise related to deposition in ancient glacial marine environments and particularly linked to ice-distal facies resulting from the Hirnantian glaciation of north Gondwana (Oggiano, Mameli, 2006; Couto et al., 2013).

CONCLUSIONS

The described fibrous microfabrics in Upper Ordoician glaciomarine diamictites record the synkinematic growth of antitaxial strain fringes between rigid objects and rock matrix as a result of diffusive mass-transfer processes associated with progressive deformation. The relatively simple fringe geometry and fiber orientation as well as the limited occurrence of quartz and chamosite strain fringes indicate a single phase of locally manifested deformation under low temperature conditions. In view of the spatial occurrence of tectonic structures in exposed Lower Palaeozoic strata across the study area (Ivanov, 1970), the timing of the deformation event could be broadly related to the Variscan orogeny. This conclusion is supported by the statement of Boncheva et al. (2010) that all marine Palaeozoic (Ordovician to Lower Carboniferous) sedimentary rocks of the Balkan Terrane were affected by the Variscan orogeny during the Carboniferous. This study documents a rare case of strain fringes developed in non-metamorphosed sedimentary rocks and is likely to be the first one reporting strain fringes in diamictites and chamosite mineralogy of beard overgrowths.

Acknowledgments

The author is thankful to V. Vangelova and K. Bogdanov (Sofia University “St. Kliment Ohridski”) for kindly assisting with the performed chemical analyses. The colleagues N. Georgiev, N. Bonev, and Y. Gerdzhikov (Sofia University “St. Kliment Ohridski”) made very helpful comments on the manuscript. This study was financially supported by the Science Fund of Sofia University – Project 3/2012.

REFERENCES

Angelov, V., Antonov, M., Gerdzhikov, S., Tanatsiev, S., Kiselinov, H., Petrov, P., Valev, V. 2010. *Geological map of the Republic of Bulgaria 1:50 000. Map sheet Litakovo*. Apis 50, Sofia.

Angelov, V., Antonov, M., Gerdzhikov, S., Sirakov, V., Tanatsiev, S., Sachanski, V., Valev, V. 2011. *Geological map of the Republic of Bulgaria 1:50 000. Map sheet Svoge*. Apis 50, Sofia.

Boncheva, I., Lakova, I., Sachanski, V., Koenigshof, P. 2010. Devonian stratigraphy, correlations and basin development in the Balkan Terrane, Western Bulgaria. *Gondwana Research* 17, 573-582.

Bons, P.D., Elburg, M.A., Gomez-Rivas, E. 2012. A review of the formation of tectonic veins and their microstructures. *Journal of Structural Geology* 43, 33-62.

Chatalov, A., Vangelov, D., Sachanski, V., Tanatsiev, S. 2014. Upper Ordovician diamictites from the Balkan Terrane, Western Bulgaria: A glaciomarine record of the Gondwana Hirnantian glaciation. *Buletini i Shkencave Gjeologogjike, 2, Special Issue Proceedings of XX CBGA Congress, Tirana*, 276-277.

Couto, C., Knight, J., Lourenço, A. 2013. Late Ordovician ice-marginal processes and sea-level change from the north Gondwana platform: Evidence from the Valongo Anticline (northern Portugal). *Palaeogeography, Palaeoclimatology, Palaeoecology* 375, 1-15.

Dewers, T., Ortoleva, P. 1991. Influences of clay minerals on sandstone cementation and pressure solution. *Geology* 19, 1045-1048.

Durney, D.W., Kisch, H.J. 1994. A field classification and intensity scale for first-generation cleavages. *AGSO Journal of Australian Geology and Geophysics* 15, 257-295.

Ghosh, D., Dutta, T., Samanta, S.K., Pal, D.C. 2013. Texture, microstructure and geochemistry of magnetite from the Banduhurang uranium mine, Singhbhum shear zone, India: Implications for physico-chemical evolution of magnetite mineralization. *Journal Geological Society of India* 81, 101-112.

Goldhaber, M.B. 2005. Sulfur-rich sediments. In: Mackenzie, F.T. (Ed.), *Sediments, diagenesis, and sedimentary rocks: Treatise on Geochemistry* 7. Elsevier–Pergamon, Oxford, 257-288.

Gray, D.R. 1978. Cleavages in deformed psammitic rocks from Southeastern Australia: Their nature and origin. *Geological Society of America Bulletin* 89, 577-590.

Gutiérrez-Marco, J.C., Yanev, S.N., Sachanski, V.V., Rábano, I., Lakova, I., San José Lancha, M.A., Diéz Martínez, E., Boncheva, I., Sarmiento, G.N. 2003. New biostratigraphical data from the Ordovician of Bulgaria. *INSUGEO, Serie Correlacion Geologica* 17, 79-85.

Ivanov, Z. 1970. On the nature and sequence of early deformations in the Lower Paleozoic rocks of Stara planina Mountains between Iskar River valley and Etropole pass. *Proceedings of the Geological Institute, series Geotectonics* 19, 25-59 (in Bulgarian, with Russian and French abstracts)

Ivanov, Z. 1998. Tetctonics of Bulgaria. Habilitation thesis. Sofia University “St. Kliment Ohridski”, Sofia, 634 pp. (in Bulgarian).

Koehn, D., Hilgers, C., Bons, P.D., Passchier, C.W. 2000. Numerical simulation of fibre growth in antitaxial strain fringes. *Journal of Structural Geology* 22, 1311-1324.

Lafrance, B., Vernon, R.H. 1998. Coupled mass transfer and microfracturing in gabbroic mylonites. In: Snoke, A.W., Tullis, J., Todd, V.R. (Eds.), *Fault-related rocks: A photographic atlas*. Princeton University Press, Princeton, 204-207.

Lakova, I., Sachanski, V. 2004. Cryptospores and trilite spores in oceanic graptolite-bearing sediments (Saltar Formation) across the Ordovician–Silurian boundary in the West Balkan Mountains, Bulgaria. *Review of the Bulgarian Geological Society* 65, 151-156.

Liu, K.W. 2002. Deep-burial diagenesis of the siliciclastic Ordovician Natal Group, South Africa. *Sedimentary*

Geology 154, 177-189.

Means, W.D. 1975. Natural and experimental microstructures in deformed micaceous sandstones. *Geological Society of America Bulletin* 86, 1221-1229.

Meere, P.A., Mulchrone, K.F. 2006. Timing of deformation within Old Red Sandstone lithologies from the Dingle Peninsula, SW Ireland. *Journal of the Geological Society London* 163, 461-469.

Merriman, R.J., Peacor, D.R. 1999. Very low-grade metapelites: Mineralogy, microfabrics and measuring reaction progress. In: Frey, M., Robinson, D. (Eds.), *Low-grade metamorphism*. Blackwell Science, Oxford, 10-60.

Moore, D.M., Reynolds, R.C. 1997. *X-ray diffraction and the identification and analysis of clay minerals (2nd edition)*. Oxford University Press, Oxford–New York, 378 pp.

Oggiano, G., Mameli, P. 2006. Diamictite and oolitic ironstones, a sedimentary association at Ordovician–Silurian transition in the north Gondwana margin: New evidence from the inner nappe of Sardinia Variscides (Italy). *Gondwana Research* 9, 500-511.

Passchier, C.W., Trouw, R.A.J. 2005. *Microtectonics (2nd revised edition)*. Springer-Verlag, Berlin–Heidelberg–New York, 366 pp.

Perri, F. 2008. Clay mineral assemblage of the Middle Triassic-Lower Jurassic mudrocks from western-central Mediterranean Alpine Chains. *Periodico di Mineralogia* 77, 23-40.

Ramsay, J.G., Huber, M.I. 1983. *The techniques of modern structural geology, Volume 1: Strain analysis.* Academic Press, London, 307 pp.

Sačanski, V. 1993. Boundaries of the Silurian System in Bulgaria. *Geologica Balcanica* 23, 25-33.

Sachanski, V. 1994. Age of the Sirman Formation and Tseretsel Formation in Sofia Stara planina Mountains (Ordovician, Ashgill). *Review of the Bulgarian Geological Society* 55, 83-90 (in Bulgarian, with English abstract).

Sachanski, V., Tenchov, Y. 1993. Lithostratigraphic subdivision of the Silurian sediments in the Svoge anticline. *Review of the Bulgarian Geological Society* 54, 71-81 (in Bulgarian, with English abstract).

Tsankov, Ts. 1995. Tectonics. In: Yanev, S. (Ed.), *Explanatory notes to Geological map of Bulgaria 1:100 000. Map sheet Sofia*. Avers, Sofia, 94-107 (in Bulgarian).

van der Pluijm, B.A. 1984. Mica beards in three slates: Morphology, formation and bearing on the strain history. *Geologische Rundschau* 73, 1037-1053.

Williams, P.F. 1972. 'Pressure shadow' structures in foliated rocks from Bermagui, New South Wales. *Journal of the Geological Society of Australia* 18, 371-377.

Wintsch, R.P., Yi, K. 2002. Dissolution and replacement creep: A significant deformation mechanism in mid-crustal rocks. *Journal of Structural Geology* 24, 1179-1193.

Yanev, S. 2000. Palaeozoic terranes of the Balkan Peninsula in the framework of Pangea assembly. *Palaeogeography, Palaeoclimatology, Palaeoecology* 161, 151-177.

Yanev, S., Lakova, I., Boncheva, I., Sachanski, V. 2005. The Moesian and Balkan Terranes in Bulgaria: Palaeozoic marine basin development, palaeogeography and tectonic evolution. *Geologica Belgica* 8, 185-192.

Yanev, S., Stefanov, D. 2001. Paleozoic pelitic rocks in Bulgaria. I. Composition, genesis and postsedimentary evolution of the pelitic rrocks in Western Stara Planina. *Review of the Bulgarian Geological Society* 62, 3-10 (in Bulgarian, with English abstract).

Young, T.P., Taylor, W.E.G. (Eds.). 1989. Phanerozoic Ironstones. *Geological Society London, Special Publications* 46, 251 pp.

Printed 2015